Structural Engineering and Mechanics, Vol. 20, No. 1 (2005) 1-20
DOI: http://dx.doi.org/10.12989/sem.2005.20.1.001

Seismic response and failure modes for a water storage structure – A case study

Kapilesh Bhargava†

Engineering Services Group, Bhabha Atomic Research Centre, Trombay, Mumbai 400 085, India

A. K. Ghosh‡

Health Safety and Environment Group, Bhabha Atomic Research Centre, Trombay, Mumbai 400 085, India

S. Ramanujam‡

Engineering Services Group, Bhabha Atomic Research Centre, Trombay, Mumbai 400 085, India

(Received November 26, 2004, Accepted February 25, 2005)

Abstract. The present paper deals with the seismic response analysis and the evaluation of most likely failure modes for a water storage structure. For the stress analysis, a 3-D mathematical model has been adopted to represent the structure appropriately. The structure has been analyzed for both static and seismic loads. Seismic analysis has been carried out considering the hydrodynamic effects of the contained water. Based on the stress analyses results, the most likely failure modes viz. tensile cracking and compressive crushing of concrete for the various structural elements; caused by the seismic event have been investigated. Further an attempt has also been made to quantify the initial leakage rate and average emptying time for the structure during seismic event after evaluating the various crack parameters viz. crack-width and crack-spacing at the locations of interest. The results are presented with reference to peak ground acceleration (PGA) of the seismic event. It has been observed that, an increase in PGA would result in significant increase in stresses and crack width in the various structural members. Significant increase in initial leakage rate and decrease in average emptying time for the structure has also been observed with the increase in PGA.

Key words: tension/compression zone; cracking; crushing; crack-width; crack-spacing; seismic; tank; water; failure.

1. Introduction

In the context of stress analysis, the assessment of the most likely failure modes for the structure caused by seismic event is a very important consideration. In general, the structure is considered to fail functionally when the degree of distress in the structure due to a seismic event achieves a

† Scientific Officer, Corresponding author, E-mail: Kapil_66@magnum.barc.ernet.in
‡ Head

certain level, beyond which it would be reasonable to assume that the appropriate and designated functioning of the structure could be negatively impacted substantially. However, this degree of distress is very subjective and must reflect the location of the structural distress. Because concrete is relatively weak in tension, cracking is expected when significant tensile stresses are induced in the structural members that are beyond the permissible stress value and this can expose reinforcing steel to oxygen and moisture and make the steel more susceptible to corrosion, resulting in reduced tensile capacity of the structural members. In the case of water retaining structures, cracking may result in the leakage of water through the cracks and this problem may become very severe due to the occurrence of a seismic event. Similarly, crushing of concrete would occur when significant compressive stresses are induced in the structural members that are beyond the permissible stress value and this failure may result in spalling of concrete in the compression zone and subsequently the loss of cover to the reinforcement, making the steel more susceptible to corrosion and eventually resulting in reduced capacity of the structural members. Crushing failures are usually sudden without sufficient warning and may become catastrophic due to the occurrence of a seismic event.

The present paper is concerned with the seismic response analysis and failure mode assessment of a water-storage structure. The scope of the present work includes : (i) stress analysis of the structure for static and seismic loading and the evaluation of stresses at different locations of interest for various combinations of static and seismic loadings, (ii) assessment of the most likely failure modes for the structure during a seismic event, (iii) quantification of the crack parameters viz. crack-width and crack-spacing at the locations of interest, initial leakage rate and average emptying time for the structure during a seismic event.

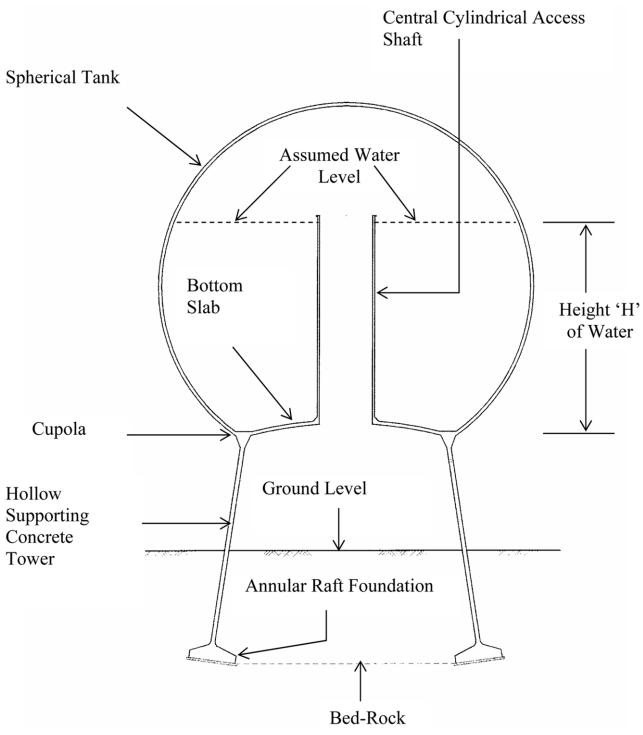

Fig. 1 Structural features of the water storage structure

Table 1 Nominal values of the relevant input data for the water-storage structure

Material Properties for the Structure (Nominal Values)	
1. Grade of concrete	= M35 (F_{ck} = 35 MPa)
2. Grade of reinforcing steel	= Fe250 (F_y = 250 MPa)
3. Poisson's ratio for concrete	= 0.15
4. Unit weight of concrete	= 25 KN/m^3
5. Structural damping for the structure	= 7%

Note : (i) F_{ck} is 28 days characteristic compressive strength of concrete.
(ii) F_Y is yield strength of reinforcing bars.

Normalized Ground Motion Response Spectral Shape Values (RSSV)									
Time period (sec.)	0.0	0.1	0.2	0.4	0.6	0.8	1.0	1.5	2.0
RSSV	1.000	2.145	2.715	2.190	1.62	1.230	1.095	0.860	0.665

2. Structural features

The present study has been carried out for a water-storage structure for which the structural features are shown in Fig. 1. The structure in question is spherical in shape filled with water and encloses a central cylindrical access shaft inside it, which extends above the top water level in the tank by about 0.15 m. The structure is supported by a hollow supporting concrete tower on an embedded annular raft foundation. The base of the annular raft foundation rests on bed rock. The nominal values of the relevant input data related to the material properties for the structure are given in Table 1.

3. Mathematical modelling

For the purpose of stress analysis, a 3-D mathematical model has been adopted to represent the structure appropriately. The structure has been modeled as an assemblage of various elements like shell, mass and spring, based on the finite element technique. The lumped mass idealization has been adopted to model the mass of the structure; wherein the lumped masses are calculated at the nodal locations by the software program by using the specified values of mass density of the material. The various structural features viz. hollow supporting concrete tower, central cylindrical access shaft and the spherical tank have been idealized as an assembly of 4-noded quadrilateral thin shell elements. Since the structure rests on bed rock; therefore, for the purpose of stress analyses the structure is assumed to be fixed at the top of the base raft. The effect of side soil around the hollow supporting concrete tower has been neglected. This is a conservative assumption. In the absence of side soil, the cantilever action of the tank structure will be more, leading to a higher seismic response, which normally dictates the structural design. Fig. 2 shows a portion of the 3-D finite element model of the structure adopted in the present study (Bhargava *et al.* 2003).

The effect of soil-structure interaction (SSI) is not considered in the present study i.e., the effect of side soil around the hollow supporting concrete tower has been neglected. In principle, the SSI will change the time period of the structure and modify its seismic response. In a separate study, the present authors have shown that the effect of SSI for this particular structure is not very significant (Bhargava *et al.* 2002) and therefore may be ignored.

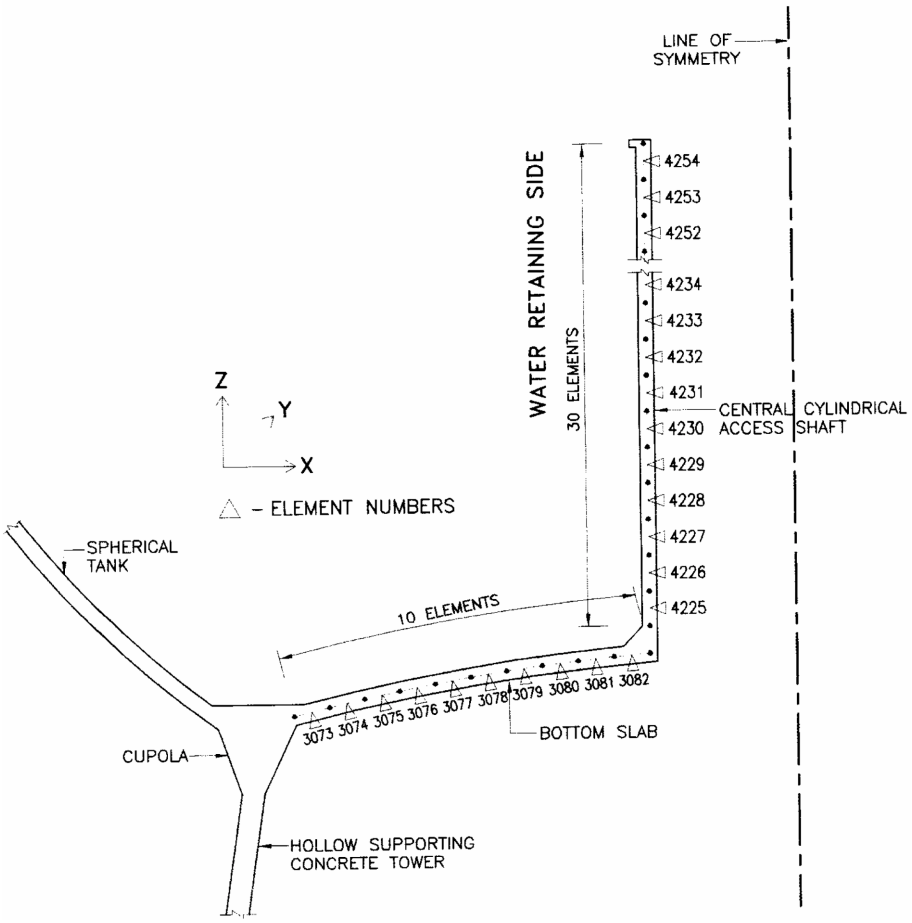

Fig. 2 Portion of 3-D finite element model of the water storage structure

4. Fluid-structure interaction

The tank structure has been analyzed for the dynamic effects of the seismic ground motion. When a tank containing water is subjected to base excitation; the pressures exerted by the water on the tank change in intensity and distribution from those corresponding to a state of static equilibrium. The resulting hydrodynamic pressures vary with time and induce time-dependant stresses in the tank which may affect its performance. These pressures and stresses depend on the characteristics of the excitation, the properties of the contained water, and the geometrical and physical properties of the tank itself. For a horizontally excited tank for which the liquid surface is free, a portion of the liquid along the walls and the bottom moves synchronously with the tank as a rigid attached mass, while the remaining part moves independently, experiencing sloshing oscillations about a horizontal axis normal to the direction of the excitation. The hydrodynamic pressures associated with the two types of motion are distributed differently over the tank height and have different temporal variations. The pressures induced by the rigid attached mass component are maximum near the tank base and are characterized by high frequency oscillations, whereas those induced by sloshing component are

maximum at the liquid surface and are associated with low frequency oscillations.

The modeling of hydrodynamic effects and seismic response evaluation of water storage structures are still the subject of active research and have been studied by many researchers. Both experimental and theoretical studies related to the vibration of liquid storage containers have been reported in the literature. Dynamic characteristics of the liquid containers fixed at the base and free at the top have been studied by considering virtual mass due to liquid and neglecting the sloshing effects (Arya *et al*. 1971). Earthquake response of a liquid storage tank has been evaluated by assuming the tank system as a cantilever beam (Veletsos and Yang 1974). In the same study, the fluid inertial effect was considered by means of an added mass and the study was restricted to impulsive mode only. Finite element analysis of an annular cylindrical tank with an axisymmetric elastic dome has been studied by Balendra (1979). The fluid was considered as inviscid and incompressible while, the sloshing effect has been neglected. The dynamic characteristics of a ground supported cylindrical tank due to earthquake has been studied using finite element technique by treating the fluid part analytically (Housner and Haroun 1981, Haroun and Housner 1982). Sukenobu *et al*. (1982) have demonstrated the coupling phenomenon between the shell and the liquid; wherein the authors considered the liquid inside the tank in the form of an added mass. A finite element analysis to the predict the sloshing displacements and the hydrodynamic pressures in liquid filled tanks subjected to earthquake motion has been presented by Aslam (1981). The effects of water-shell interaction on the dynamic properties of fixed base steel cylinders has been studied both experimentally and theoretically by Maheri *et al*. (1991). Analytical techniques to evaluate the seismic response of vertical tanks are described in some of the references (Veletsos *et al*. 1990, Bandyopadhyay *et al.* 1996). A finite element numerical scheme to predict sloshing displacements

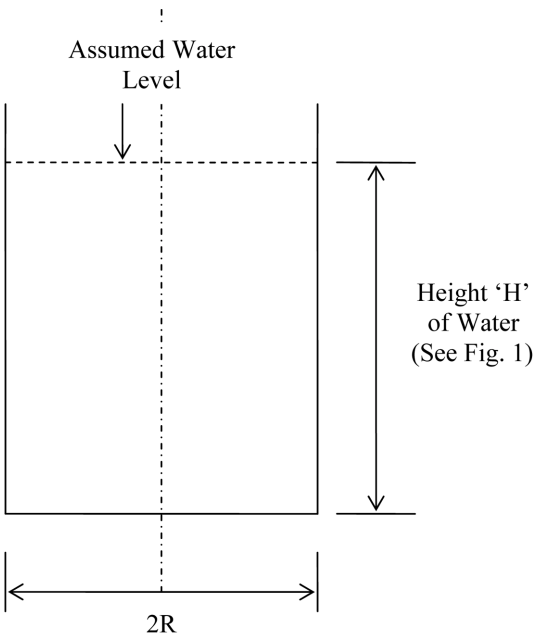

‘R’ : Radius of Equivalent Cylinder

Fig. 3 Equivalent cylindrical geometry of the spherical tank

and hydrodynamic pressures in thin walled liquid retaining structures due to external excitation has been presented by Babu *et al*. (1996). Various codes of practice have provisions to account for hydrodynamic effects under seismic excitation (USAEC 1963, ASCE 1998).

The majority of above-ground fluid-containing vertical tanks do not warrant a sophisticated finite element hydrodynamic fluid-structure interaction analysis for a seismic loading (ASCE 1998). Therefore, in the present study the hydrodynamic effects of the water contained within the tank have been modeled as per reference (USAEC 1963) and accordingly the calculated horizontal masses (i.e., impulsive mass and sloshing mass with associated horizontal spring constant) and vertical mass of the water were attached at appropriate nodes of the finite element model of the structure (Bhargava *et al.* 2003). For the sake of simplification, the masses and spring constants due to hydrodynamic effects have been calculated by converting the spherical geometry to an equivalent cylindrical geometry. Fig. 3 shows the equivalent cylindrical geometry of the spherical tank; wherein the radius 'R' of the cylindrical geometry has been evaluated by keeping the volume and height of water same, in both the spherical and cylindrical tanks.

5. Stress analyses of the present structure

5.1 Static analysis

The static analysis has been carried out for various design loads that include self-weight of the structure and hydrostatic pressure due to available water inside the tank structure. The software program COSMOS/M (1997) has been used for static analysis.

5.2 Dynamic analysis

The structural response to the earthquake ground motion is evaluated using the response spectrum technique and the software program COSMOS/M (1997) has been used for this purpose. The

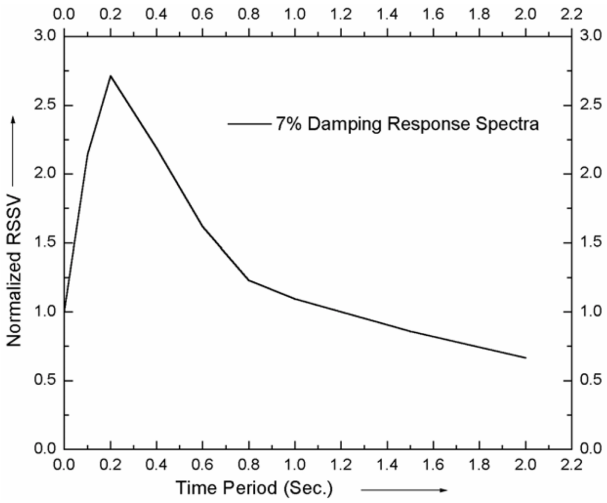

Fig. 4 Normalized seismic ground motion response spectra

seismic input includes two horizontal and the vertical components of the ground motions in combination (ASCE 1998). The spectral acceleration for the vertical ground motion has been taken as 0.67 times the value for horizontal ground motion (ASCE 1998). The maximum response of the structure has been obtained by using the CQC method for modal combination and the spatial combination has been performed using the square root of sum of squares (SRSS) technique (ASCE 1998). Seismic analysis of the structure (Bhargava *et al.* 2003) has been carried out by using the nominal response spectral shape values as given in Table 1. Fig. 4 shows the plot of the normalized seismic ground motion response spectrum used in the present study.

5.3 Assumptions in stress evaluation

The following assumptions are made for the evaluation of stresses in various structural members:

(i) The stress evaluation for the structural members is based on the linear elastic theory which implies that at any cross section, plane sections before bending remain plane after bending, and this in turn means that unit strains above and below the neutral axis are proportional to the distance from the neutral axis.

(ii) The stress evaluation in the structural members is done by considering the grosssectional properties of the member i.e., the cross-section of the member ignoring the allowance of reinforcing steel area in terms of equivalent concrete units. This assumption permits simple calculation on a homogeneous basis. However, from design point of view this is a conservative assumption.

(iii) In the stress calculations relating to the resistance to cracking, the entire section of the concrete including the cover participates in resisting the direct and flexural loads or combination of both.

5.4 Stress evaluation for structural members

The output results of the static and dynamic analyses have been combined for the purpose of stress evaluation. Since no signs are associated with the output results of dynamic analysis due to the SRSS spatial combination, the possibility of various load combinations for the output results of static and seismic loadings were explored to have conservatism on the overall structural response. It may be noted that, the structural reinforced concrete walls are designed in accordance with the recommendations given for structural reinforced concrete columns subjected to axial load and uniaxial moment, in each of the horizontal and vertical directions (BIS 2000). Therefore, considering this philosophy for the design of structural reinforced concrete walls, the following four load combinations were explored for the purpose of conservatism on the overall structural response.

$$\text{i. Load Combination 1 (LC1)} : [N_d + N_e],\ \text{ABS}[M_d + M_e] \quad (1)$$

$$\text{ii. Load Combination 2 (LC2)} : [N_d + N_e],\ \text{ABS}[M_d - M_e] \quad (2)$$

$$\text{iii. Load Combination 3 (LC3)} : [N_d - N_e],\ \text{ABS}[M_d + M_e] \quad (3)$$

$$\text{iv. Load Combination 4 (LC4)} : [N_d - N_e],\ \text{ABS}[M_d - M_e] \quad (4)$$

Here, N_d and N_e are axial loads for the wall element due to static and earthquake loads while M_d and M_e are moments for the wall element due to static and earthquake loads. The stress evaluations for central cylindrical shaft and bottom slab were carried out for the load combinations as mentioned by Eqs. (1) to (4) and this in turn resulted in the evaluation of extreme fiber bending

compressive and bending tensile stresses for all the elements as shown in the Fig. 2.

The results are presented with reference to normalized peak ground acceleration (PGA_N) and normalized stress (S_N) values. 'PGA_N' is defined as the ratio of any PGA to the design basis PGA and 'S_N' is defined as the ratio of actual evaluated stress value from numerical analyses to the permissible bending tensile stress value for concrete from the resistance to cracking consideration. For concrete, the permissible bending compressive stress value from resistance to strength consideration and permissible bending tensile stress value from resistance to cracking consideration are considered as 11.5 MPa and 2.2 MPa respectively as per the reference literature (BIS 1965).

Figs. 5(a), 5(b), 5(c) and 5(d) present the vertical stress distribution along height of the central cylindrical shaft at inner water face and outer face of the shaft for different values of PGA_N for load combinations LC1, LC2, LC3 and LC4 respectively. Figs. 6(a), 6(b), 6(c) and 6(d) present the

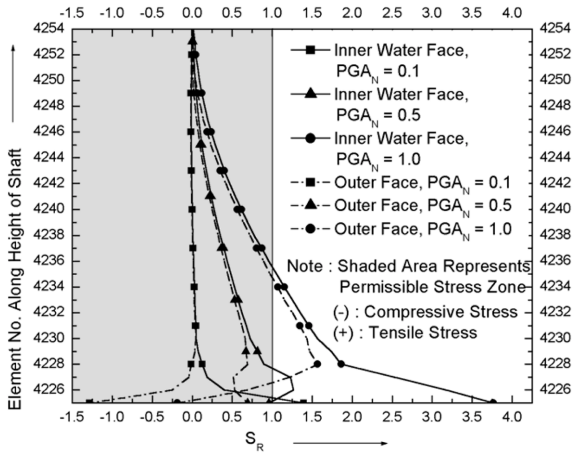

Fig. 5(a) Vertical stress distribution along the height of shaft for load combination 'LC1'

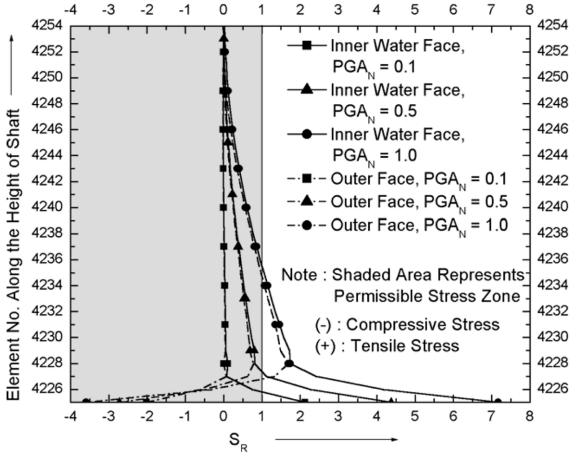

Fig. 5(b) Vertical stress distribution along the height of shaft for load combination 'LC2'

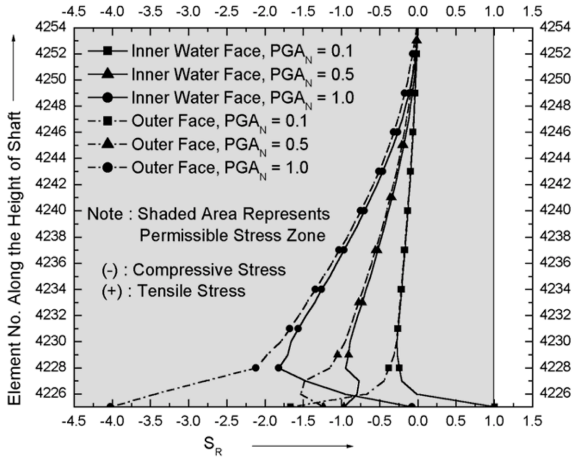

Fig. 5(c) Vertical stress distribution along the height of shaft for load combination 'LC3'

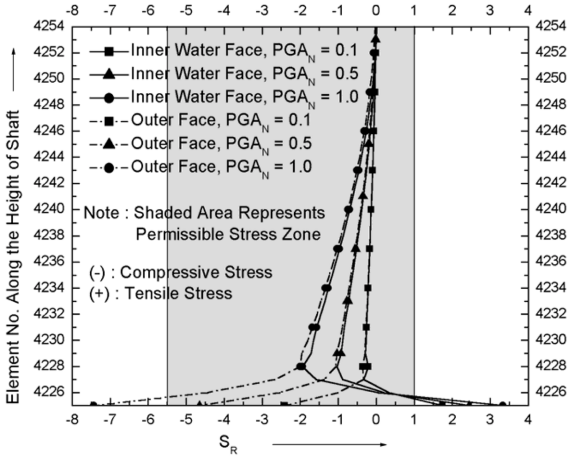

Fig. 5(d) Vertical Stress distribution along the height of shaft for load combination 'LC4'

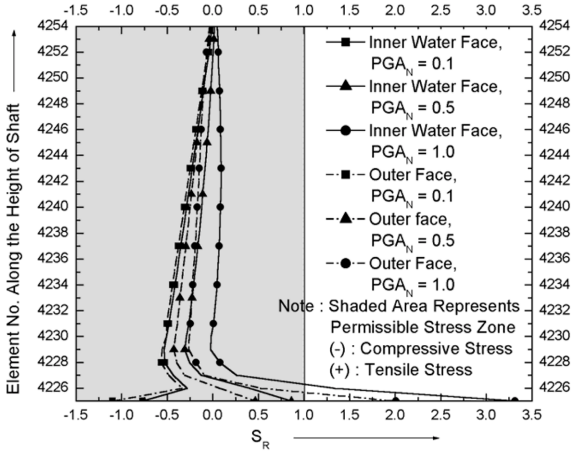

Fig. 6(a) Circumferential stress distribution along the height of shaft for load combination 'LC1'

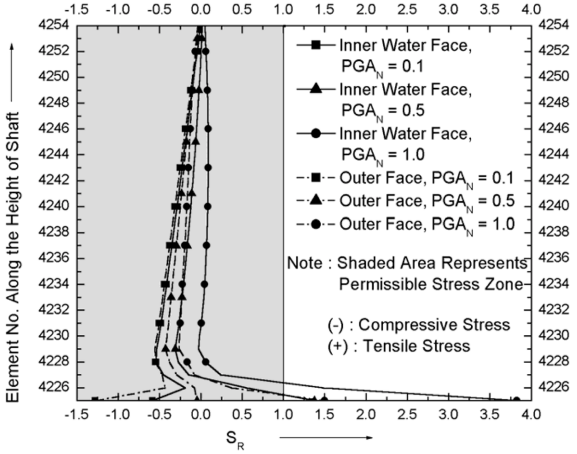

Fig. 6(b) Circumferential stress distribution along the height of shaft for load combination 'LC2'

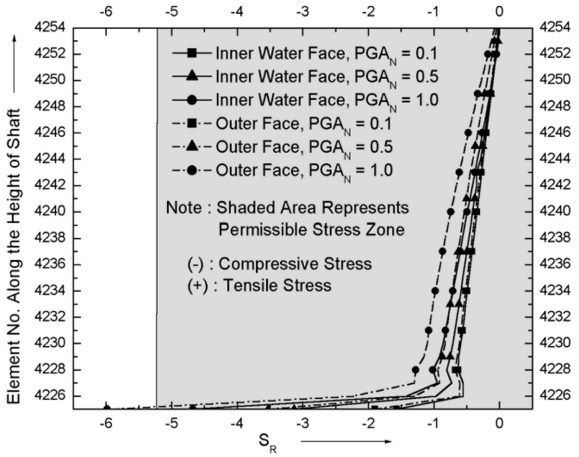

Fig. 6(c) Circumferential stress distribution along the height of shaft for load combination 'LC3'

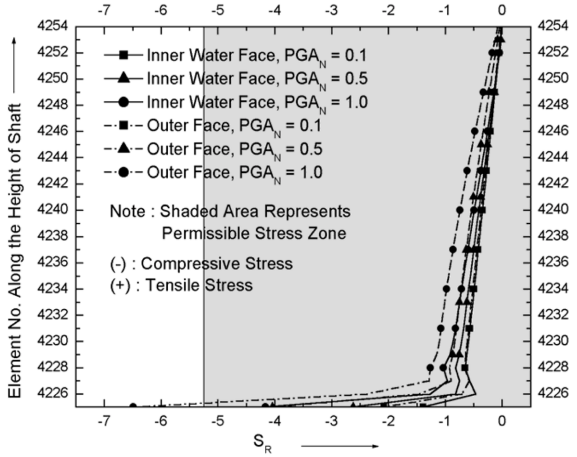

Fig. 6(d) Circumferential stress distribution along the height of shaft for load combination 'LC4'

circumferential stress distribution along the height of the central cylindrical shaft at inner water face and outer face of the slab for different values of PGA_N for load combinations LC1, LC2, LC3 and LC4 respectively.

Figs. 7(a), 7(b), 7(c) and 7(d) present the radial stress distribution along length of the bottom slab at inner water face and outer face of the slab for different values of PGA_N for load combinations LC1, LC2, LC3 and LC4 respectively. Figs. 8(a), 8(b), 8(c) and 8(d) present the circumferential stress distribution along the length of the bottom slab at inner water face and outer face of the slab for different values of PGA_N for load combinations LC1, LC2, LC3 and LC4 respectively.

Figs. 9(a) and 9(b) present the tension/compression zones for the central cylindrical shaft and bottom slab, respectively, as a function of PGA_N with reference to 'Z_L'. Here, it may be stated that the tension/compression zones are the areas which correspond to the portions of the central

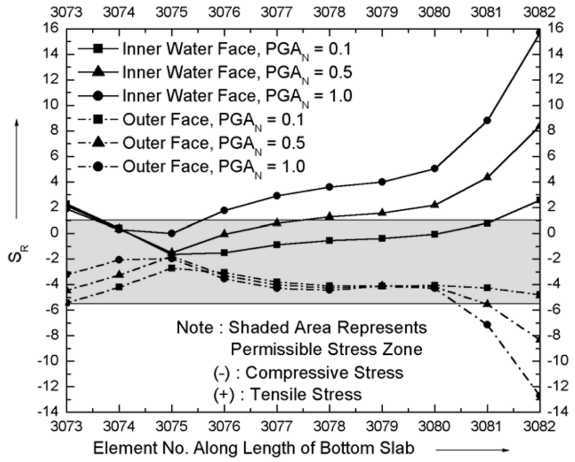

Fig. 7(a) Radial stress distribution along the length of bottom slab for load combination 'LC1'

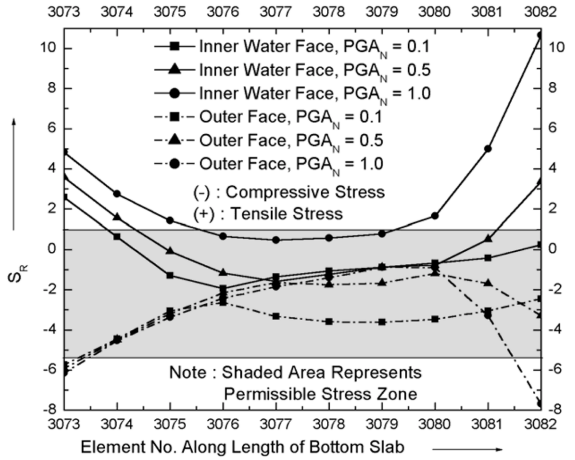

Fig. 7(b) Radial stress distribution along the length of bottom slab for load combination 'LC2'

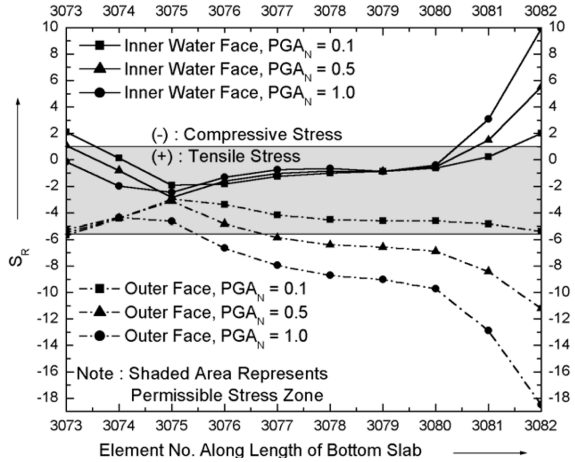

Fig. 7(c) Radial stress distribution along the length of bottom slab for load combination 'LC3'

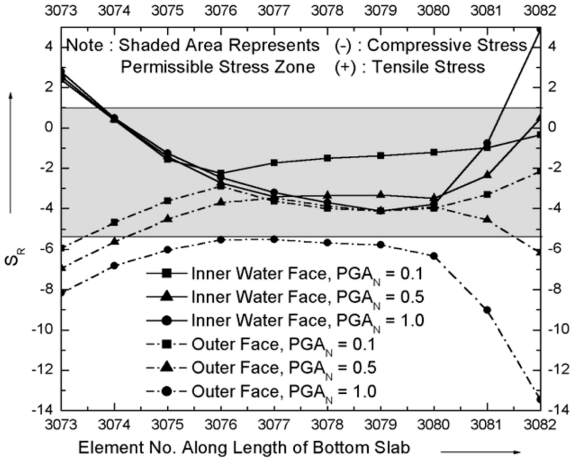

Fig. 7(d) Radial stress distribution along the length of bottom slab for load combination 'LC4'

cylindrical shaft and the bottom slab where the actual stresses from numerical analyses are beyond permissible stress values, and 'Z_L' is defined as the ratio of length/height corresponding to the tension/compression zone to the total length/height for the structural members.

6. Assessment of failure modes

Based on the stress analyses results it would be reasonable to assume that, under seismic excitation, the structure essentially behaves like a cantilever beam with circular cross-section, somewhat modified by the rocking of the base raft. Therefore, it would be appropriate to assume bending of the structure in the direction of seismic ground motion as a dominant mode of failure, and this will result in the linear variation of the bending stresses across the cross-section, as long as

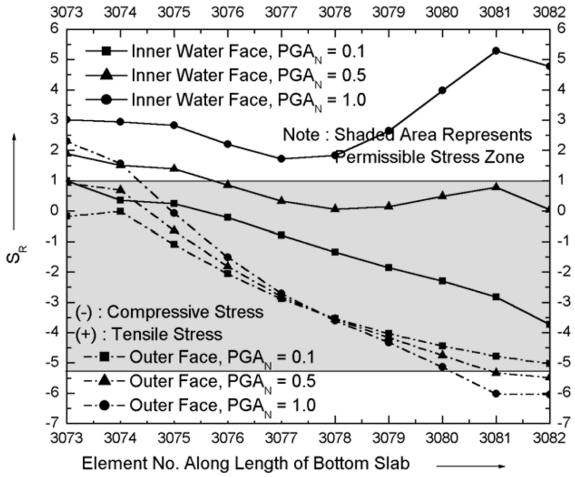

Fig. 8(a) Circumferential stress distribution along the length of bottom slab for load combination 'LC1'

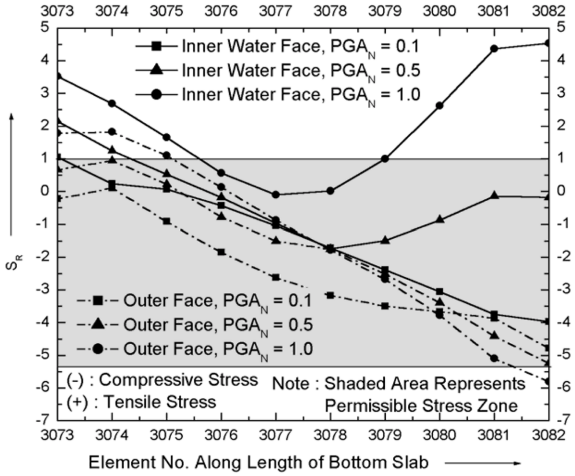

Fig. 8(b) Circumferential stress distribution along the length of bottom slab for load combination 'LC2'

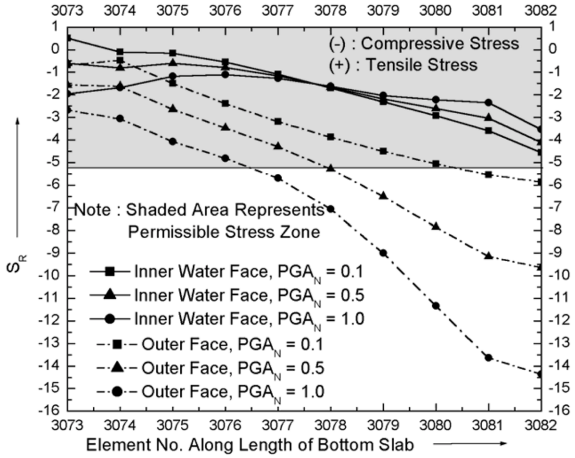

Fig. 8(c) Circumferential stress distribution along the length of bottom slab for load combination 'LC3'

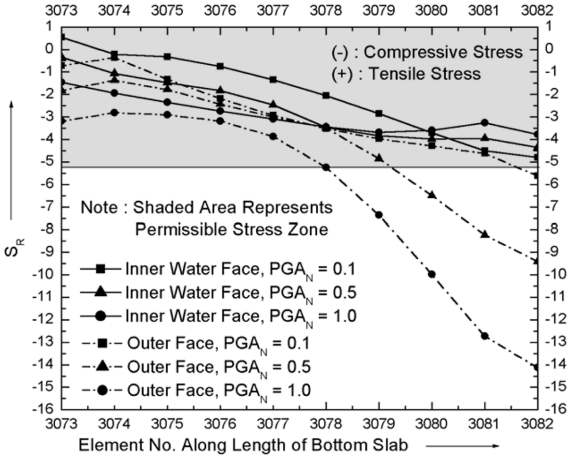

Fig. 8(d) Circumferential stress distribution along the length of bottom slab for load combination 'LC4'

the response of the structure stays in the elastic range. The structure is considered to fail when the bending stress in the structural members due to a given seismic event achieves the maximum permissible stress value at the location of interest.

It is evident from the Figs. 5 to 8 that the stresses along the height of the central cylindrical shaft and along the length of the bottom slab increase substantially with PGA_N. Similarly, it is observed from Figs. 9(a) and 9(b) that, with the increase in PGA_N value, there is a marked increase in tension/compression zones. Based on the stress analyses of the present structure, two failure scenarios have been observed : (i) cracking of concrete due to tension and (ii) crushing of concrete due to compression. Since the stress evaluation for the structural members is based on linear elastic

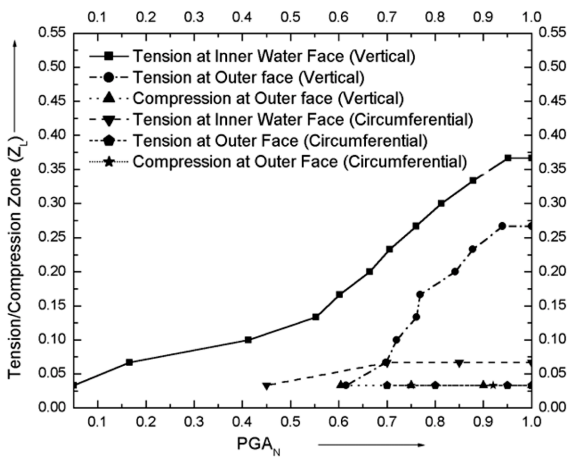

Fig. 9(a) Propagation of tension/compression zones in shaft as a function of PGA_N

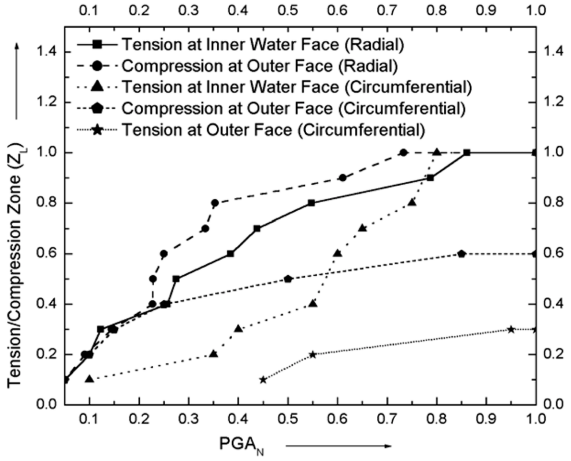

Fig. 9(b) Propagation of tension/compression zones in bottom slab as a function of PGA_N

theory, the failure scenarios are assumed to occur as soon as the evaluated stresses achieve the maximum permissible stress values in the present study, and this would result in reasonable conservatism in the seismic analysis and design.

It is clear from Figs. 5 and 6 that, except for a very small portion near to the bottom slab, the stress distribution along height of the central cylindrical shaft is nearly membrane and this would result in the entire cross-section experiencing either compressive or tensile stresses. Therefore in the portion where the evaluated extreme fiber tensile stresses are beyond the permissible stress value on both the inner water face and the outer face of the shaft, there would be through thickness cracking in that portion of shaft. Similarly in the portion where the evaluated extreme fiber compressive stresses are beyond the permissible stress value on both the inner water face and the outer face of the shaft, there would be loss of strength due to crushing of concrete in that portion of shaft. It is also evident from Figs. 7 and 8 that the stress distribution along length of the bottom slab is mainly flexural, and this would result in both compressive and tensile stresses being generated across the thickness of bottom slab. Therefore there will be partial local cracking of the cross section where the evaluated bending tensile stresses are beyond the permissible stress values on the inner water face of the bottom slab, and there will be local loss of strength over part of the cross-section where the evaluated bending compressive stresses are beyond the permissible stress values on the outer face of the bottom slab. However, it may be mentioned here that these assumptions pertaining to through thickness cracking, local cracking, and local loss of strength in the central cylindrical shaft and bottom slab would result in reasonable conservatism as far as the structural design is concerned.

6.1 Cracking of concrete due to tension

Reinforced concrete tension members generally have cracks penetrating completely through the cross-section and steel reinforcement is the only connecting link between the various parts, while on the other hand reinforced concrete flexural members have cracks in the tensile zone only and they penetrate only a part of the cross-section. In the present study, for the sake of simplicity, the structural members subjected to tension with negligible eccentricity are assumed to fail when the

evaluated tensile stress across the cross-section achieves the permissible stress value and this would further result in the through thickness cracking across the entire cross-section. Similarly, the structural members subjected to axial loads with large and considerable eccentricity are assumed to fail when the evaluated extreme fiber bending tensile stress achieves the permissible stress value and this would further result in the partial cracking of the cross-section in tension zone only.

6.1.1 Central cylindrical shaft

6.1.1.1 Vertical direction

The formation of a tension zone in the central cylindrical shaft as a function of PGA_N in the vertical direction is presented in Figs. 5 and 9(a). These figures depict the following:

(a) For a PGA_N value of 0.05, around 4% height of the central cylindrical shaft will have tension zones on the inner water face and this would result in the formation of cracks at the inner water face of the shaft that would penetrate only a part of the cross-section.
(b) With the increase in PGA_N value, there will be an increase in the tension zone along height of shaft on the inner water face.
(c) For the PGA_N value of 1.0, around 37% of the height of the shaft will have a tension zone on its inner water face.
(d) For a PGA_N value of about 0.62, the shaft will have tension zones on both the inner and outer faces and this would result in the beginning of formation of through thickness cracks in the shaft.
(e) For the PGA_N value of 1.0, around 27% of the height of the shaft will have tension zones on both the inner and outer faces resulting in through thickness cracks.

6.1.1.2 Circumferential direction

The formation of a tension zone in the central cylindrical shaft as a function of PGA_N in the circumferential direction is presented in Figs. 6 and 9(a). These figures depict the following:

(a) For a PGA_N value of 0.45, around 4% of the height of the central cylindrical shaft will have tension zones on the inner water face and this would result in the formation of cracks at the inner water face of the shaft that would penetrate only a part of the cross-section.
(b) With the increase in PGA_N value, there will be an increase in the tension zone along the height of shaft on the inner water face.
(c) For the PGA_N value of 1.0, around 7% of the height of the shaft will have a tension zone on its inner water face.
(d) For a PGA_N value of about 0.7, the shaft will have tension zones on both the inner and outer faces and this would result in the beginning of formation of through thickness cracks in the shaft.
(e) For the PGA_N value of 1.0, around 4% of the height of the shaft will have tension zones on both the inner and outer faces resulting in through thickness cracks.

6.1.2 Bottom slab

6.1.2.1 Radial direction

The formation of a tension zone in the bottom slab as a function of PGA_N in the radial direction is presented in Figs. 7 and 9(b). These figures depict the following:

(a) For a PGA_N value of 0.05, around 10% of the length of the bottom slab will have tension zones on the inner water face and this would result in the formation of cracks at the inner

water face that would penetrate only a part of the cross-section.

(b) With an increase in the PGA_N value, there will be an increase in the tension zone along the length of bottom slab on the inner water face.

(c) For a PGA_N value of 0.86, the whole length of the bottom slab will have a tension zone on its inner water face, and this trend continues until the PGA_N reaches a value of 1.0. Also, the bottom slab would not have through thickness cracking for any value of PGA_N, as no portion of the bottom slab experiences tension zones on both the inner and outer faces.

6.1.2.2 Circumferential direction

The formation of a tension zone in the bottom slab as a function of PGA_N in the circumferential direction is presented in Figs. 8 and 9(b). These figures depict the following:

(a) For a PGA_N value of 0.1, around 10% of the length of the bottom slab will have tension zones on the inner water face and this would result in the formation of cracks at the inner water face that would penetrate only a part of the cross-section.

(b) With an increase in the PGA_N value, there will be an increase in the tension zone along the length of bottom slab on the inner water face.

(c) For a PGA_N value of 0.8 the whole length of the bottom slab will have a tension zone on its inner water face and this trend continues until the PGA_N reaches a value of 1.0.

(d) For a PGA_N value of about 0.55, the bottom slab will have tension zones on both the inner and outer faces and this would result in the beginning of formation of through thickness cracks in the shaft.

(e) For the PGA_N value of 1.0, around 30% length of the bottom slab will have tension zones on both the inner and outer faces resulting in through thickness cracks.

6.2 Crushing of concrete due to compression

In reinforced concrete compression members, the failure occurs as soon as the steel yields and the surrounding concrete develop its maximum permissible compressive strength. In the present study, for the sake of simplicity, the structural members subjected to compression with negligible eccentricity are assumed to fail when the evaluated compressive stress across the cross-section achieves the maximum permissible stress value and this would further result in the crushing of concrete across the entire crosssection. In reinforced concrete flexural members, the concrete fails suddenly in a somewhat brittle fashion as soon as the full strength of concrete is developed in the compression zone. It may be noted that, in the case of flexural members, if the amount of steel is small then steel yielding will take place before the concrete attains its maximum capacity and similarly if the amount of steel is large then concrete would attain its maximum capacity before steel yielding takes place. In the present study for the sake of simplicity, the structural members subjected to axial loads with large and considerable eccentricity are assumed to fail when the evaluated extreme fiber bending compressive stress achieves the maximum permissible stress value and this would further result in the crushing of concrete in the compression zone only.

6.2.1 Central cylindrical shaft

6.2.1.1 Vertical direction

The formation of a compression zone in the central cylindrical shaft as a function of PGA_N in the vertical direction is presented in Figs. 5 and 9(a). These figures depict the following:

(a) For a PGA_N value of 0.6, around 4% of the height of the central cylindrical shaft will have a compression zone on its outer face and the same trend continues until the PGA_N reaches a value of 1.0. Therefore, for the shaft a very small portion of height would be susceptible to crushing of concrete in the compression zone.

6.2.1.2 Circumferential direction

The formation of a compression zone in the central cylindrical shaft as a function of PGA_N in the circumferential direction is presented in Figs. 6 and 9(a). These figures depict the following:

(a) For a PGA_N value of 0.75, around 4% of the height of the central cylindrical shaft will have a compression zone on its outer face and the same trend continues until the PGA_N reaches a value of 1.0. Therefore, for the shaft a very small portion of height would be susceptible to crushing of concrete in the compression zone.

6.2.2 Bottom slab

6.2.2.1 Radial direction

The formation of a compression zone in the bottom slab as a function of PGA_N in the radial direction is presented in Figs. 7 and 9(b). These figures depict the following:

(a) For a PGA_N value of 0.05, around 10% of the length of the bottom slab will have compression zones at the outer face and this would result in the initiation of crushing of concrete at the outer face of the bottom slab.
(b) With an increase in the PGA_N value, there will be an increase in the compression zone along the length of the bottom slab on the outer face.
(c) For a PGA_N value of 0.73, the whole length of the bottom slab will have a compression zone on its outer face, and the same trend continues until the PGA_N reaches a value of 1.0. Also, the bottom slab would not have through thickness crushing for any value of PGA_N, as no portion of the bottom slab experiences compression zones on both the inner and outer faces.

6.2.2.2 Circumferential direction

The formation of a compression zone in the bottom slab as a function of PGA_N in the circumferential direction is presented in Figs. 8 and 9(b). These figures depict the following:

(a) For a PGA_N value of 0.05, around 10% of the length of the bottom slab will have compression zones at the outer face and this would result in the initiation of crushing of concrete at the outer face of the bottom slab.
(b) With an increase in the PGA_N value, there will be an increase in the compression zone along the length of the bottom slab on the outer face.
(c) For a PGA_N value of 0.85, around 65% of the length of the bottom slab will have a compression zone at its outer face and the same trend continues until the PGA_N reaches a value of 1.0. Also, the bottom slab would not have through thickness crushing for any value of PGA_N, as no portion of the bottom slab experiences compression zones on both the inner and outer faces.

7. Treatment of cracks

For water storage structures, cracking may be detrimental to the durability of the structural

members and therefore crack control assumes significant importance if one has to design a water storage structure in a rational and economic manner. Several codes of practice have extensive provisions (BIS 2000, CEB-FIP 1990, ACI 1985) for crack width, crack spacing and crack control, which are indeed the basic aspects of cracking. It may be noted that, the useful purpose of crack-width and crack-spacing formulae is to aid the designer in choosing a particular mode of detailing in preference to the other equally practicable modes. Cracks would allow the leakage of water through them and this would further result in the weakening of bond between reinforcement and concrete, corrosion of reinforcement, and the reduced structural capacity of the various structural members of a water storage structure, and this problem may become very severe if one has to reassess an existing structure for a seismic event. In the present study, the evaluation of crack-width, crack-spacing, leakage rate of water from the tank structure, and average emptying time for the structure during a seismic event have been carried out. It has been assumed that the leakage of water would take place from the through-thickness cracked portions of the shaft and bottom slab during a seismic event.

7.1 Formulations for crack-width and crack-spacing

Prediction of crack-width and crack-spacing has been studied by many researchers (Broms 1965, Broms *et al*. 1965, Gergely *et al*. 1968, Beeby 1979, Macgregor *et al*. 1980, Rizkallah *et al*. 1984(a) (b), Chowdhary *et al*. 1997, 2001). Several codes of practice also have extensive provisions for crack width, crack spacing and crack control (BIS 2000, CEB-FIP 1990, ACI 1985). However, despite these efforts, a widely accepted methodology for predicting crack-width and crack-spacing has not yet been established because available formulations for evaluation of crack-width and crack-spacing present a wide scatter of predicted values. It may be noted that, the present study is not intended to compare the evaluated crack-width and crack-spacing using different available formulae, rather it basically aims to quantify the leakage rate and average emptying time for the present structure. Therefore keeping this in mind, the crack-width has been evaluated using reference (BIS 2000) and mean crack-spacing has been evaluated using reference (ACI 1990) and these references are widely accepted among international community.

The following assumptions are made in the evaluation of crack-width : (i) the concrete and steel are both considered being fully elastic in tension and compression, (ii) the elastic modulus of steel is taken as 200 KN/mm^2 and (iii) the elastic modulus of concrete is taken as 5700 $(f_{ck})^{0.5}$ both in compression and tension and where, f_{ck} is the 28 days cube compressive strength of concrete.

Provided that the strain in the tension reinforcement is limited to 0.8 *Fy/Es*, the design surface crack-width and mean crack-spacing are calculated from Eqs. (5) and (6).

$$W_{cr} = \frac{3 \times a_{cr} \times \varepsilon_m}{1 + \dfrac{2 \times (a_{cr} - C_{\min})}{h - x}} \tag{5}$$

$$S_{rm} = 2.0 \times (C_{\min} + s/10) + k_2 \times k_3 \times \frac{d_b}{Q_R} \tag{6}$$

where,

a_{cr} = Distance from the point considered to the surface of the nearest longitudinal bar,

$C_{\min}$ = Minimum cover to the longitudinal bar,

ε_m = Average steel strain at the level considered,
h = Overall depth of the member, and
x = Depth of the neutral axis.
s = Bar spacing, limited to $15d_b$,
k_2 = 0.4 for ribbed bars,
k_3 = Depends on the shape of the stress diagram, 0.125 for bending,
d_b = Bar diameter,
Q_R = A_s/A_t
A_t = Effective area of cross-section in tension, depending on arrangement of bars and type of external forces, it is limited by a line not more than halfway to the neutral axis,
A_s = Area of tension reinforcement.

7.2 Evaluation of crack-width, crack-spacing, initial leakage-rate and average emptying time for structure

After the stress evaluation, the crack-widths and crack-spacing have been evaluated using Eqs. (5) and (6) for central cylindrical shaft and bottom slab of the structure for each of the four load combinations as defined by Eqs. (1) to (4) for all the elements at different PGA_N values. The maximum crack width among those evaluated for the four load combinations has been further used to evaluate the initial leakage rate and the average emptying time for the tank through the structure in the case of a seismic event. It is noted that, cracks that open due to stresses during a seismic event are likely to close after the seismic event. Therefore, the calculated leakage rate and the average emptying time are thus very conservative. It may also be noted that crack-widths have been evaluated on both the inner water face and the outer face of shaft and bottom slab for PGA_N values ranging from 0.62 to 1.0 for the shaft and 0.55 to 1.0 for the bottom slab due to the presence of a tension zone on both of the faces, and this would further result in through-thickness cracking of the shaft. For other values of PGA_N ranging from 0.05 to 0.62 for the shaft and 0.05 to 0.55 for the bottom slab, both will have a tension zone at the inner water face only, and accordingly the crack-widths have been evaluated on that face and this would further result in partial-thickness cracking of the shaft and the bottom slab. However, the partial-thickness cracks on the inner water face of the shaft and the bottom slab are assumed to propagate through the thickness of the shaft, and this would be a reasonable assumption in the conservative estimate of initial leakage rate and average emptying time for the structure. For the evaluation of initial leakage rate, the maximum value of crack-width among those calculated on both the inner water face and the outer face has been considered. The initial leakage rate has been evaluated based on the principles of hydraulics using Eqs. (7) and (8) as follows:

$$Q = A_C \times V_C \tag{7}$$

$$V_C = C_d \sqrt{2 \times g \times H_C} \tag{8}$$

Where,
Q = Initial leakage rate (m^3/sec.)
A_C = Area of cross-section for the crack (m^2)
V_C = Initial velocity of discharge of water (m/sec.)

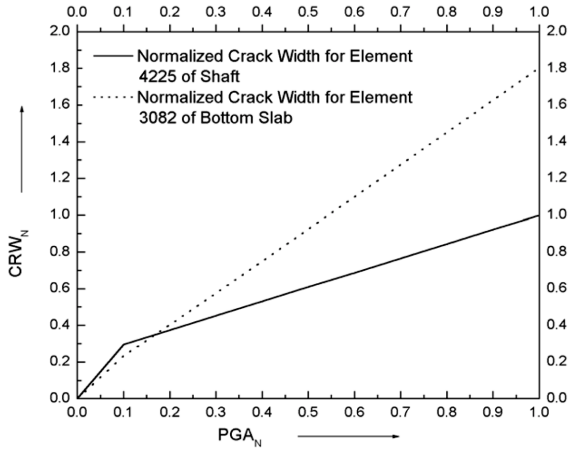

Fig. 10 Normalized crack width as a function of PGA_N at inner water face

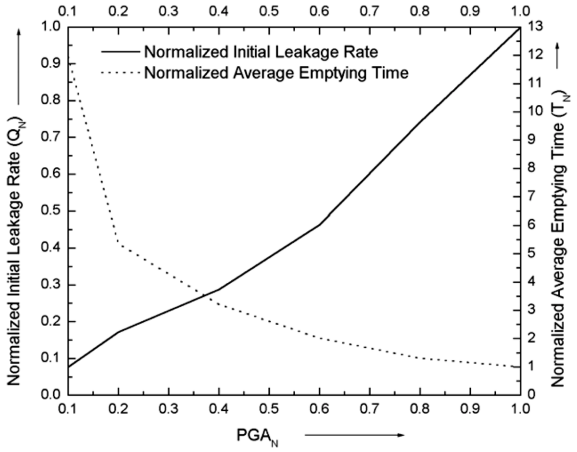

Fig. 11 Normalized initial leakage rate and normalized average emptying time for structure as a function of PGA_N

g = Acceleration due to gravity (9.81 m/sec.^{2})
H_C = Initial water head at the crack level (m)
C_d = Discharge coefficient

The results are presented with reference to normalized crack-width (CRW_N), normalized initial leakage rate (Q_N), and normalized average emptying time (T_N) for the structure. 'CRW_N' is defined as the ratio of crack-width at any PGA_N value to the crackwidth for element 4225 of shaft at a PGA_N value of 1.0. 'Q_N' is defined as the ratio of initial leakage rate at any PGA_N value to the initial leakage rate through the structure at a PGA_N value of 1.0. 'T_N' is defined as the ratio of average emptying time at any PGA_N value to the average emptying time through the structure at a PGA_N value of 1.0.

Fig. 10 presents the crack-width variation as a function of PGA_N for element 4225 of central cylindrical shaft and element 3082 of bottom slab respectively. It is evident that, with an increase in the PGA_N value, there is a marked increase in the crack-widths for the aforementioned elements. It is also clear from the same figure that the crack-width for element 3082 of the bottom slab is approximately 1.8 times the same for element 4225 at a PGA_N value of 1.0.

Fig. 11 presents the initial leakage rate and average emptying time for the structure as a function of PGA_N. It is evident that, with the increase in PGA_N value, there is marked increase in the initial leakage rate and a marked decrease in average emptying time through the structure. For a PGA_N value of 1.0, the average emptying time through the structure is approximately 10% of that for a PGA_N value of 0.05.

8. Conclusions

The Following conclusions are drawn from the present case study:

A significant increase in stresses along the height of central cylindrical shaft and the length of bottom slab has been observed with the increase in PGA_N. Similarly, with an increase in the PGA_N

value, propagation of tension/compression zones along the height of the shaft and along the length of the bottom slab assumes significant importance.

A significant increase in crack-widths and in the initial leakage rate through the shaft has been observed with an increase in the PGA_N values. Similarly, a significant decrease in average emptying time for the structure through the shaft has been observed with an increase in the PGA_N values. These trends are expected. However, the present case study brings out these trends in a quantitative way. It also shows that there is no gross collapse of the structure within the range of PGA_N considered in the present study.

This study could be very useful in the rational design of water storage structures. With the knowledge in hand of crack width and crack spacing, the designer would be in a good position to effectively select the suitable form of reinforcing detailing so as to reduce the initial leakage rate and increase the average emptying time through the structure during a seismic event. However, it may be difficult to generalize the reinforcement detailing aspect based on the present case study, since service conditions can vary from case to case. The present paper is a part of an ongoing research work to apply such failure mode analysis to prevent undesirable mode of failure for the tank structures.

The present study could be useful in evaluating the failure modes and the associated risks for similar structures, particularly for those that can not easily be strengthened. This study could also be very useful to evaluate the real safety margins available in the case of a seismic reassessment of an existing water storage structure.

References

ACI (1985), *ACI-318 : Standard Code Requirements for Reinforced Concrete and Commentary*, American Concrete Institute, Detroit, USA.

ACI (1990), *ACI-224R : Control of Cracking in Concrete Structures*, American Concrete Institute, Detroit, USA.

Arya, A.S., Thakkar, S.K. and Goyal, A.C. (1971), "Vibration analysis of thin cylindrical containers", *Proceedings ASCE EM2*, 317-331.

ASCE (1998), *ASCE 4-98 : Seismic Analysis of Safety-Related Nuclear Structures and Commentary*, Fourth Revision, American Society of Civil Engineers, Washington, USA.

Aslam, M. (1981), "Finite element analysis of earthquake induced sloshing in axisymmetric tanks", *Int. J. Numer. Meth. Engg.*, **17**, 159-169.

Babu Subhash, S. and Bhattacharyya, S.K. (1996), "Finite element analysis of fluid-structure interaction effect on liquid retaining structures due to sloshing", *Comput. Struct.*, **59**(6), 1165-1171.

Balendra, T. (1979), "Earthquake finite element analysis of an annular cylindrical liquid storage tanks", *Proc. 3rd Int. Conf. on Finite Element Methods*, Australia.

Bandyopadhyay, K., Cornell, A., Costantino, C., Kennedy, R., Miller, C. and Veletsos, A. (1995), "Seismic design and evaluation guidelines for the department of energy high-level waste storage tanks and appurtenances", Brookhaven National Laboratory Report 52361, Upton, N.Y., USA.

Beeby, A.W. (1979), "The prediction of crack widths in hardened concrete", *Structural Engineer* (London), **57A**(1), 9-17.

Bhargava Kapilesh, Ghosh, A.K. and Ramanujam, S. (2003), "Seismic response analysis of a water storage structure", *Proc. of Structural Engineering Convention, SEC 2003*, Kharagpur, India, 511-521.

Bhargava Kapilesh, Ghosh, A.K., Agrawal, M.K., Patnaik, R., Ramanujam, S. and Kushwaha, H.S. (2002), "Evaluation of seismic fragility of structures – A case study", *Nuclear Engineering and Design*, **212**(1-3), 253-272.

BIS (1965), *IS : 3370 Part II, Indian Standard Code of Practice for Concrete Structures for the Storage of*

Liquids, Part II : Reinforced Concrete Structures, Bureau of Indian Standards, New Delhi, India.
BIS (2000), *IS : 456, Indian Standard Code of Practice for Plain and Reinforced Concrete*, Fourth Revision, Bureau of Indian Standards, New Delhi, India.
Broms, B.B. (1965), "Crack width and crack spacing in reinforced concrete members", *ACI J.*, **62**(10), 1237-1256.
Broms, B.B. and Lutz, L.A. (1965), "Effects of arrangement of reinforcement on crack width and spacing of reinforced concrete members", *ACI J.*, **62**(11), 1395-1420.
CEB-FIP (1990), *Comite Euro-International du Beton-Federation International de la Precontrainte – Design Code*, Thomas Telford, London, UK.
Chowdhary, S.H. and Loo, Y.C. (1997), "Crack width formula for reinforced and partially prestressed concrete beams", *Proc., Int. Conf. on Maintenance and Durability of Concrete Structures*, Hyderabad, India, 46-51.
Chowdhary, S.H. and Loo, Y.C. (2001), "A new formula for prediction of crack widths in reinforced and partially prestressed concrete beams", *Advances in Structural Engineering – An Int. J.*, **4**(2), 101-110.
COSMOS/M 2.0 (1997), *A Complete Finite Element Analysis System*, Structural Research & Analysis Corporation, Los Angeles, USA.
Gergely P. and Lutz, L.A. (1968), "Maximum crack width in reinforced concrete flexural members – Cause, mechanism and control of cracking in concrete", *SP-20, American Concrete Institute*, Detroit, 87-117.
Haroun, M.A. and Housner, G.W. (1982), "Dynamic characteristics of liquid storage tanks", *Proceedings ASCE*, **108**, 783-799.
Housner, G.W. and Haroun, M.A. (1981), "Seismic design of liquid storage tanks", *J. Technical Council of ASCE*, USA.
Macgregor, J.G., Rizkallah, S.H. and Simmonds, S.H. (1980), "Cracking of reinforced and prestressed concrete wall segments", Structural Engineering Report, No. 82, Department of Civil Engineering, University of Alberta, Edmonton, Canada.
Maheri, M.R. and Severn, R.T. (1991), "Hydrodynamic consideration for seismic design of cylindrical structures", *Civil Engg. Dyn.*, 297-313.
Rizkallah, S.H., Lau, B.L. and Simmonds, S.H. (1984a), "Air leakage characteristics in reinforced concrete", *J. Struct. Eng.*, ASCE, **110**(5), 1149-1162.
Rizkallah, S.H. and Hwang, L.S. (1984b), "Crack prediction for members in uniaxial tension", *ACI J.*, **81**(10), 572-579.
Sukenobu Tani, Tanaka, Y. and Hori, N. (1982), "Dynamic analysis of cylindrical shells containing liquid", *J. Press. Vessel Technol.*, **104**, 1229-1234.
USAEC (1963), *Nuclear Reactors and Earthquakes* (TID-7024), US Atomic Energy Commission, Washington, USA.
Veletsos, A.S. and Shivakumar, P. (1990), "Hydrodynamic effects in tanks with different conditions of support", *Third DOE Natural Phenomena Hazards Mitigation Conference*, St. Louis, Mo., 446-455.
Veletsos, A.S. and Yang, J.Y. (1974), "Seismic effects on liquid storage tanks", *Proc. 5th World Conf. on Earthq. Eng.*, Rome.